Ultra-wideband Localization with Collocated Receivers

Ruiqing Ye and Huaping Liu

School of Electrical Engineering and Computer Science, Oregon State University, Corvallis, OR 97331 USA
E-mail: {yeru,hliu}@eecs.oregonstate.edu, +1 541 737 2973

***Abstract*—A three-dimensional (3-D) ultra-wideband time-of-arrival (TOA) localization scheme that employs a single cluster of receivers is studied in this paper. The receivers are placed in proximity (e.g., on a two-dimensional plane within a few decimeters), and thus it does not require wireless synchronization of the receivers. The optimum 3-D receiver placement in the sense of minimum estimation variance defined by the Cramér-Rao lower bound is analyzed. The position error bound as a function of the number of receivers and the distance between the source and the receiver unit is derived. A hardware and software prototype that works in the 3.1−5.1 GHz range is constructed and tested in a laboratory environment. An average position estimation error of 26.6 cm is achieved in the experiment when the transmitter is within 10 meters of the receiver unit, in which four receivers are placed within a rectangle of 85 × 70 cm^2.**

***Index Terms*—Ultra-wideband (UWB), time-of-arrival (TOA), localization, geometric dilution of precision (GDOP), position error bound (PEB).**

I. Introduction

Most of the ultra-wideband (UWB) localization systems reported so far use multiple distributed receivers, and the transmitter should be placed inside the receiver geometry [1]–[4]. A recent effort has demonstrated the feasibility of three-dimensional (3-D) UWB localization using a single receiver unit [5]. While no analysis or other technical details for such type of systems are available (neither in the one-page data sheet [5], nor in other existing literature, to our knowledge), the one reported in [5] appears to use a combination of time-of-arrival (TOA) and angle-of-arrival (AOA) techniques. Compared with other UWB localization systems, the single-receiver-unit localization system has several advantages such as simple system design and easy system setup.

The goal of this paper is to provide a comprehensive analysis of an UWB 3-D localization system that employs a single cluster of receivers placed in proximity (e.g., on a 2-D plane within a few decimeters). This system employs the TOA technique. Since the receivers are placed in proximity, the system does not need to synchronize them wirelessly.

Localization accuracy of TOA localization systems depends not only on the quality of the range measurements and the number of receivers, but also on how the receivers are arranged. This is the geometric effect that is often termed geometric dilution of precision (GDOP) [6] in geolocation literature. The effect of receiver geometric configuration on localization accuracy is studied in [6], [7].

Yang and Scheuing [8], [9] have shown that the uniform angular array (UAA) can achieve the minimum mean-square error (MSE) for a source located inside the geometry in time-difference-of-arrival (TDOA) positioning. Ji and Liu [10] studied the array geometry for energy based localization that can minimize the source position MSE and reached the same conclusion that the solution is a UAA. Schroeder [11] extends the theoretical optimum receiver placement to practical applications by minimizing the average GDOP. This derivation is based on the assumption that the source node (transmitter) is inside the receiver geometry configuration. When the transmitter is away from the receivers, the 2-D optimum receiver geometry for TOA, AOA, TDOA localization with decoupled range and bearing estimation is analyzed in [12].

In this paper we analyze optimum receiver placement for a 3-D localization system with collocated receivers in the sense of minimum estimation variance defined by the Cramér-Rao lower bound (CRLB) [13], and derive the position error bound (PEB) as a function of the number of receivers and the distance between the transmitter and the receiver unit. We also construct a hardware and software prototype system that works in the 3.1−5.1 GHz range, and test it in a laboratory environment to validate the analysis results. We show with experimental results that with four receivers placed within a square of side length of 8.5 decimeters, the average error (distance between estimated and actual positions) for sources that within 10 meters from the receiver unit is within three decimeters.

II. System Model

Consider a system with all receivers placed inside a small receiver box. The coordinates of all M receivers expressed as $\mathbf{Q} = [\mathbf{q}_1, \mathbf{q}_2, \cdots \mathbf{q}_M]$ are known, where $\mathbf{q}_i = [x_i, y_i, z_i]^T$ represents the $\{x, y, z\}$-coordinates of the ith receiver. The unknown coordinate $\mathbf{p} = [x, y, z]^T$ of a transmitter are to be estimated. Since the receivers are located in proximity, they are synchronized via wire connection. With TOA, the transmitter still needs to be synchronized with the receiver unit, but this is much easier to achieve than synchronizing many distributed receivers and the transmitter wirelessly.

Without loss of generality, the first receiver is designated as the master node. The master node sends a ranging request to the transmitter and records a time stamp t_0 when the ranging request departs. Upon receiving the ranging request, the transmitter will transmit an UWB signal to all receivers. Assuming that the signal processing time in the transmitter is known and fixed, the TOA of the signal from the transmitter to all the receivers could be calculated. The estimated distance $\hat{d}_i$ between the transmitter and the ith receiver is modeled as

$$\begin{aligned}\hat{d}_i &= d_i + b_i + n_i \\ &= \|\mathbf{p} - \mathbf{q}_i\| + b_i + n_i, i = 1, \cdots, M\end{aligned} \tag{1}$$

where $d_i = \|\mathbf{q}_i - \mathbf{p}\|$ is the actual distance between the ith receivers and the transmitter ($\|.\|$ denotes ℓ_2 norm), b_i is a positive bias caused by non-line-of-sight (NLOS) propagation and n_i is a Gaussian variable with zero mean and variance σ^2. We only consider the LOS case; thus $b_i = 0$. For 3-D localization with TOA, we need at least four range estimates to obtain an unambiguous position estimate. However, if the receiver unit is placed in the same plane and the transmitter is always located on one side of this plane, then three range estimates are sufficient. One example of this system model is shown in Fig. 1, where all the receivers are placed in the same plane. For indoor applications, the receiver unit could be mounted on a wall or a ceiling.

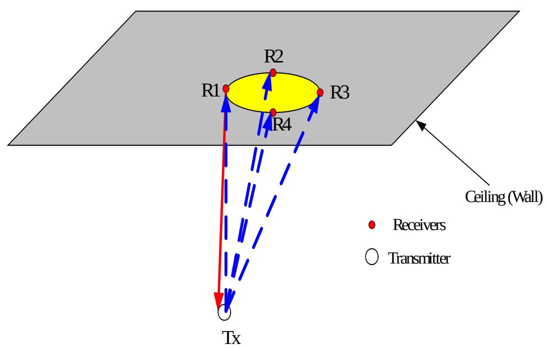

Fig. 1. Illustration of the system configuration.

III. Optimum Receiver Geometry

In this section, we analyze the optimum receiver geometry for the system described in Sec. II. The criterion is the minimum estimation variance defined by the CRLB derived under an additive Gaussian noise model.

A. Cramér-Rao Lower Bound for TOA Localization

CRLB is a lower bound for the variance of an unbiased estimator. It is often used as a benchmark for estimation performance. Let the M independent range estimates obtained by the M receivers be $\hat{\mathbf{d}} = [\hat{d}_1, \hat{d}_2, \cdots, \hat{d}_M]$ with corresponding mean values $\mathbf{d} = [d_1, d_2, \cdots, d_M]$ and the same variance σ^2. The CRLB can be written as [15]

$$\mathbf{J}^{-1} = \sigma^2(\mathbf{G}\mathbf{G}^T)^{-1} \tag{2}$$

where $\mathbf{J}$ is the Fisher information matrix (FIM) and $\mathbf{G} = [\mathbf{g}_1, \mathbf{g}_2, ..., \mathbf{g}_N]$ with

$$\mathbf{g}_i = \frac{\mathbf{p} - \mathbf{q}_i}{\|\mathbf{p} - \mathbf{q}_i\|}. \tag{3}$$

One of the criteria to optimize the receiver geometry is to minimize the trace of the CRLB, which can be written as

$$\min_{\boldsymbol{g}_i} f_{\text{CRLB}} = \mathtt{tr}\left[\mathbf{J}^{-1}\right] = \sigma^2 \mathtt{tr}\left[(\mathbf{G}\mathbf{G}^T)^{-1}\right] \tag{4}$$

where $\mathtt{tr}$ denotes the trace. We assume that the range estimation error is Gaussian distributed with the same variance. Because σ^2 does not affect the receiver geometry optimization, for simplicity, we let $\sigma = 1$.

B. Optimum Receiver Geometry

The system configuration is as follows.

1) The receivers must lie on or inside a circle with a radius L, and the center of the circle is designated as the origin. Since the value of L does not affect the receiver geometry optimization, we let $L = 1$ for simplicity.
2) The number of receivers is $M \geq 3$.
3) The transmitter is assumed to be orthogonal to the plane formed by the receivers.

Based on these assumptions, the position of the ith receiver can be written as $\mathbf{q}_i = [l_i \cos\alpha_i, l_i \sin\alpha_i, 0]^T$, where α detotes the angle from the receivers to the origin and $l_i \leq L$. we set the transmitter position as $p = [0, 0, d]^T$, where d is the distance from the transmitter to the receiver plane . The FIM is written as

$$\mathbf{J} = \begin{bmatrix} \frac{\sum_{i=1}^{M} l_i^2 \cos^2\alpha_i}{1+d^2} & \frac{\sum_{i=1}^{M} l_i^2 \cos\alpha_i \sin\alpha_i}{1+d^2} & \frac{\sum_{i=1}^{M} -dl_i \cos\alpha_i}{1+d^2} \\ \frac{\sum_{i=1}^{M} l_i^2 \cos\alpha_i \sin\alpha_i}{1+d^2} & \frac{\sum_{i=1}^{M} l_i^2 \sin^2\alpha_i}{1+d^2} & \frac{\sum_{i=1}^{M} -dl_i \sin\alpha_i}{1+d^2} \\ \frac{\sum_{i=1}^{M} -dl_i \cos\alpha_i}{1+d^2} & \frac{\sum_{i=1}^{M} -dl_i \sin\alpha_i}{1+d^2} & \frac{Md^2}{1+d^2} \end{bmatrix}. \tag{5}$$

We wish to minimize $\mathtt{tr}[\mathbf{J}^{-1}]$. When $d \neq 0$, $\mathbf{J}$ is a positive definite symmetric matrix, which has several useful properties [14] that we can exploit:

1) The diagonal entries $J_{i,i}$ are real and positive.
2) $\mathtt{tr}[\mathbf{J}] > 0$.
3) $|J_{i,j}| \leq \sqrt{J_{i,i}J_{j,j}} \leq \frac{1}{2}(J_{i,i} + J_{j,j})$.

The determinant of $\mathbf{J}$ is expressed as

$$|\mathbf{J}| = J_{1,1}(J_{2,2}J_{3,3} - J_{2,3}^2) - J_{1,2}^2 J_{3,3} - J_{1,3}^2 J_{2,2} + 2J_{1,2}J_{1,3}J_{2,3} \tag{6}$$

and the first diagonal element of the inverse matrix $\mathbf{J^{-1}}$, $\mathbf{J^{-1}_{(1,1)}}$, is expressed as

$$\mathbf{J^{-1}_{(1,1)}} = \frac{(J_{2,2}J_{3,3} - J_{2,3}^2)}{J_{1,1}(J_{2,2}J_{3,3} - J_{2,3}^2) - (J_{1,2}^2 J_{3,3} + J_{1,3}^2 J_{2,2} - 2J_{1,2}J_{1,3}J_{2,3})} \tag{7}$$

We can prove that the second term of the denominator of $\mathbf{J^{-1}_{(1,1)}}$ is always greater than or equal to zero:

$$\begin{aligned} & J_{1,2}^2 J_{3,3} + J_{1,3}^2 J_{2,2} - 2J_{1,2}J_{1,3}J_{2,3} \\ & \geq J_{1,2}^2 J_{3,3} + J_{1,3}^2 J_{2,2} - |2J_{1,2}J_{1,3}J_{2,3}| \\ & \geq J_{1,2}^2 J_{3,3} + J_{1,3}^2 J_{2,2} - \left|2J_{1,2}J_{1,3}\sqrt{J_{2,2}J_{3,3}}\right| \\ & = (|J_{1,2}|\sqrt{J_{3,3}} - |J_{1,3}|\sqrt{J_{2,2}})^2 \geq 0, \end{aligned} \tag{8}$$

where we have applied the the property of a positive definite symmetric matrix, which results in $|J_{2,3}| \leq \sqrt{J_{2,2}J_{3,3}}$, in the second step.

Therefore,

$$\mathbf{J^{-1}_{(1,1)}} \geq \frac{(J_{2,2}J_{3,3} - J_{2,3}^2)}{J_{1,1}(J_{2,2}J_{3,3} - J_{2,3}^2)} = \frac{1}{J_{1,1}}. \tag{9}$$

Similarly, we can prove that

$$\mathbf{J^{-1}_{(2,2)}} \geq \frac{1}{J_{2,2}}, \tag{10a}$$

$$\mathbf{J^{-1}_{(3,3)}} \geq \frac{1}{J_{3,3}}. \tag{10b}$$

From Eqs. (9) and (10), we conclude that $\mathtt{tr}[\mathbf{J}^{-1}]$ is minimized when $J_{i,j}=0, i\neq j$, and

$$\mathbf{J}=\begin{bmatrix}\frac{\sum_{i=1}^{M} l_i^2\cos^2\alpha_i}{1+d^2} & 0 & 0\\ 0 & \frac{\sum_{i=1}^{M} l_i^2\sin^2\alpha_i}{1+d^2} & 0\\ 0 & 0 & \frac{Md^2}{1+d^2}\end{bmatrix}. \tag{11}$$

The minimum of $\mathtt{tr}[\mathbf{J}^{-1}]$ is thus obtained as

$$\begin{aligned}\mathtt{tr}[\mathbf{J}^{-1}] &= \frac{1+d^2}{\sum_{i=1}^{M} l_i^2\cos^2\alpha_i}+\frac{1+d^2}{\sum_{i=1}^{M} l_i^2\sin^2\alpha_i}+\frac{1+d^2}{Md^2}\\ &= \frac{(1+d^2)\sum_{i=1}^{M} l_i^2}{(\frac{\sum_{i=1}^{M} l_i^2}{2})^2-(\frac{1}{2}\sum_{i=1}^{M} l_i^2\cos 2\alpha_i)^2}+\frac{(1+d^2)}{Md^2}\\ &\geq \frac{4(1+d^2)}{\sum_{i=1}^{M} l_i^2}+\frac{(1+d^2)}{Md^2}\\ &\geq \frac{4(1+d^2)}{ML^2}+\frac{(1+d^2)}{Md^2}\\ &= \frac{4(1+d^2)}{M}+\frac{(1+d^2)}{Md^2}.\end{aligned} \tag{12}$$

The last equality holds when $\sum_{i=1}^{M}\cos 2\alpha_i=0$ and $l_i=L$. Therefore, the sufficient conditions that minimize $\mathtt{tr}[\mathbf{J}^{-1}]$ are

$$l_i = L = 1, i = 1, 2, \cdots M \tag{13a}$$

$$\sum_{i=1}^{M}\sin 2\alpha_i=0,\ \sum_{i=1}^{M}\cos 2\alpha_i=0 \tag{13b}$$

$$\sum_{i=1}^{M}\sin \alpha_i=0,\ \sum_{i=1}^{M}\cos \alpha_i=0. \tag{13c}$$

It is easy to show that UAA geometry is the optimum receiver geometry for this single-unit 3-D localization system.

IV. PEB When the Transmitter is Placed on a Line Orthogonal to the Receiver Plane

We have derived the sufficient conditions to determine the optimum receiver geometry. In this section, we analyze the PEB of the single-unit TOA localization system.

We consider the case when the transmitter is located at $\mathbf{p}=[0,0,d]^T$ $(d>0)$. The system configuration is illustrated in Fig. 2.

We have proved that the UAA geometry is the optimum geometry when $p=[0,0,d]^T$. Therefore, when the optimum geometry is used, the CRLB as a function of the distance d and the number of receivers M can be written as

$$\mathbf{J^{-1}}=\left(\frac{\sigma}{L}\right)^2\begin{bmatrix}\frac{2(1+d^2)}{M} & 0 & 0\\ 0 & \frac{2(1+d^2)}{M} & 0\\ 0 & 0 & \frac{1+d^2}{Md^2}\end{bmatrix}. \tag{14}$$

The PEB is thus expressed as

$$\mathrm{PEB}(\mathbf{d})=\sqrt{\mathrm{tr}[\mathbf{J}^{-1}]}=\frac{\sigma}{L}\sqrt{(\frac{4d^4+5d^2+1}{Md^2})}. \tag{15}$$

The PEB expression in Eq. (15) is a convex function of d and the minimum PEB $=\frac{\sigma}{L}\frac{9}{M}$ is reached when $d=\frac{\sqrt{2}}{2}$. In

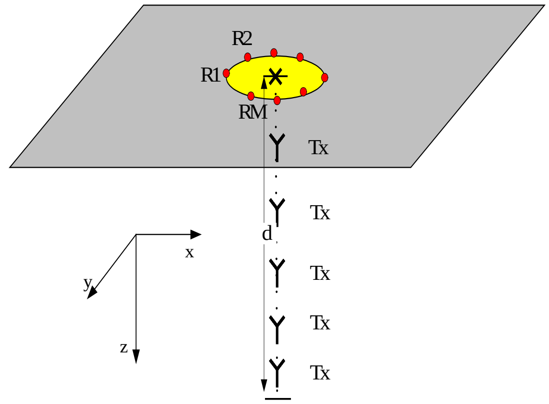

Fig. 2. Receiver configuration.

addition, the PEB decreases as the number of receivers, M, increases. The PEB versus the distance d and the number of receivers M will be simulated with the following parameters: the diameter of the localization receiver unit is $2L=1$ m, the number of receivers, M, equals $4, 6,$ and 8, and $\sigma=0.01$ m. The simulation results are shown in Fig. 3 and Fig. 4.

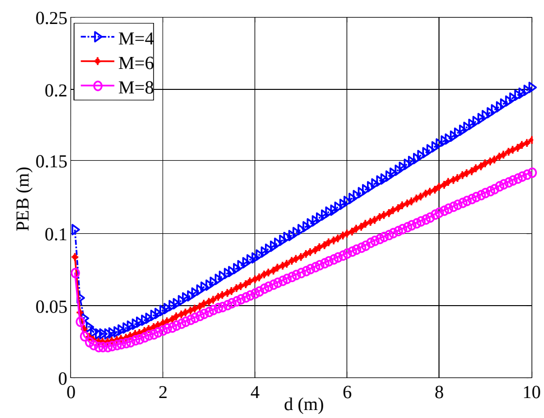

Fig. 3. PEB vs the distance as a function of the number of receivers.

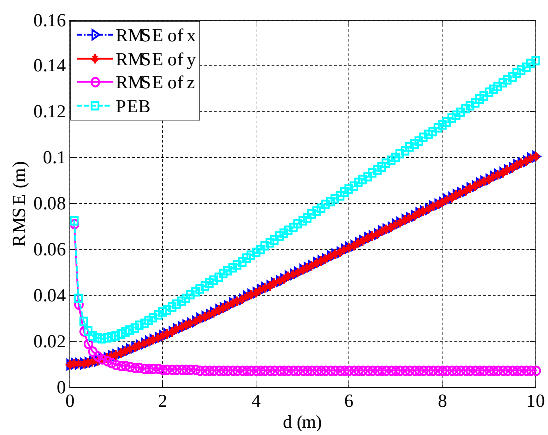

Fig. 4. Comparison of RMSE of x, y and z coordinates and PEB ($M=8$).

Fig. 3 shows how the PEB varies with the distance d and the number of receivers M. Information such as what localization accuracy the system can achieve given a set of values of M and d, or how many receivers and how big the unit need to be to achieve a certain localization accuracy could be easily obtained from this result. For example, when the diameter of the localization unit is $2L = 1$ m, $d = 10$ m, $M = 8$, and $\sigma = 0.01$ m, the PEB ≈ 0.14 m.

Fig. 4 shows the RMSE of the x, y and z coordinates when $M = 8$. Due to symmetry of x and y coordinates, the RMSEs of the x and y coordinates are identical and they increase as d increases. However, the RMSE of the z coordinate decreases as the distance d increases. The RMSE of x, y and z has a crossing point at $d = \frac{\sqrt{2}}{2}$. This provides useful information about where to put the localization unit when the accuracy requirement of the x, y and z coordinates are not the same. For example, to track the movement of people in an indoor area, for which the estimation accuracy of x and y coordinates is more important than that of the z coordinate, placing the receiver unit on the ceiling will not be the best choice.

V. Experimental Results

In order to further evaluate the performance of the single-receiver-unit 3-D localization system in a realistic setting that various inaccuracies are included, we have constructed a hardware and software prototype system and tested this system a laboratory environment.

A. Experiment Setup

The block diagram of the prototype system is shown in Fig. 5; it consists of an arbitrary waveform generator (AWG) that generates a carrier-modulated Gaussian pulse with center frequency of 4.1 GHz and -10 dB bandwidth of 2 GHz. The pulse duration is about 1 ns and the pulse repetition interval is 200 ns. An UWB omni-directional transmit antenna is connected to the pulse generator via a long coaxial cable. The length of the coaxial cable is about 50 feet, which allows the transmit antenna to be moved anywhere inside the lab. The receiver unit consists of four omni-directional antennas, wideband low-noise amplifiers, bandpass filters and a digital sampling scope.

The triggering signal from the AWG is used to trigger the sampling scope via a coaxial cable. The delay between the transmitter and the receivers is 28.64 ns. Therefore, the transmitter and the receivers are synchronized by subtracting this fixed reference delay.

The sampling scope has a maximum real-time sampling rate of 20 GHz (i.e., a sampling duration of 50 ps) for all four channels; therefore, the Nyquist sampling criterion is satisfied even when the signal is not down-converted to the baseband. The sampling scope has the capability to average over several received waveforms for noise reduction. To reduce noise effects, 20 sequentially received pulses are averaged and then recorded in a computer through an Ethernet connection.

The digital data is first upsampled to 100 GHz to increase the time resolution to 10 ps. Then it goes through a square-law device and a low-pass filter to recover the baseband pulse. The TOA between the transmitter and the four receivers are calculated using a range-estimation method that we have developed recently [4]. This method has the capability to reduce the multipath overlap effect. The position of the transmitter is calculated using the least-square method.

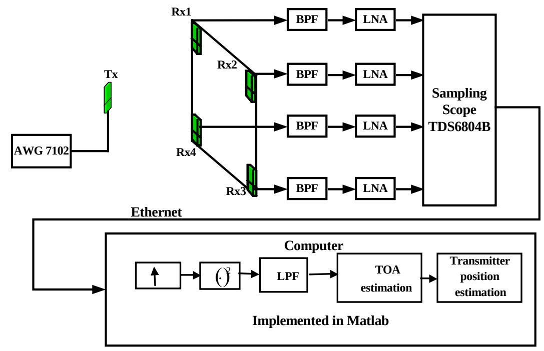

Fig. 5. Block diagram of the experimental apparatus.

B. Results

Inside the lab, there are tables between the transmitter and the receiver unit, and metal cabinets and a metal stand are along the wall, emulating a realistic multipath scenario. The four receivers are placed inside a box which is attached on a wall. One of the corners of the lab is designated as the origin and the coordinates of the four receivers are measured to be Rx1(153,23,177), Rx2(153,23,247), Rx3(238,23,247), Rx4(238,23,177). The four receivers are placed on the same plane, forming a rectangle of dimension 85 cm $\times$ 70 cm. Measurements are made at 36 different locations at a fixed height (to the floor) on the edge of a 6 m $\times$ 4.8 m rectangle with 60 cm spacing between the measurement points. The height of the measurement points is fixed at 203 cm from the floor, which ensures that the transmitting signal is not blocked by the table and metal stands in the room. The x and y coordinates of the measurement points change from 190 cm to 790 cm and from 276 cm to 756 cm, respectively. The positions of the measurement points and the receivers are shown in Fig. 6.

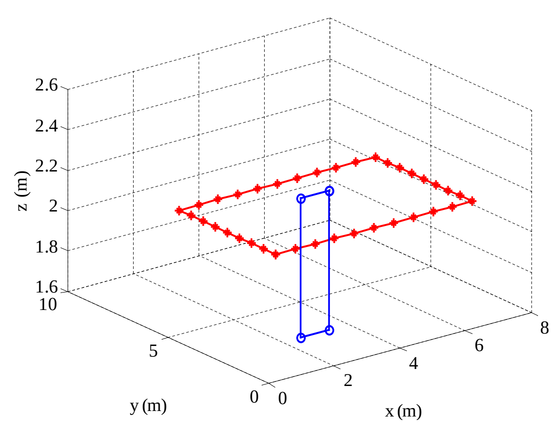

Fig. 6. Position of the measurement points and receivers in the experiment.

At each measurement point, 100 pulses are recorded by each receiver. The average TOA between the transmitter to each receiver and the position estimation at each point is estimated. Fig. 7 shows the actual and estimated positions of the 36 points.

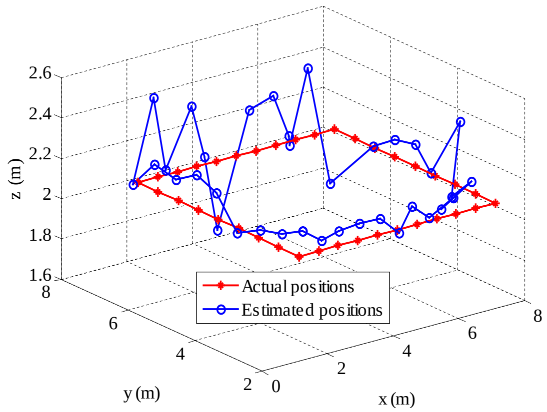

Fig. 7. Actual and estimated positions of the measurement points.

In order to further investigate the localization accuracy, the 3-D position error is calculated using

$$\epsilon_i = \|\hat{\mathbf{p}}_\mathbf{i} - \mathbf{p}_\mathbf{i}\| \tag{16}$$

where $\mathbf{p}_\mathbf{i}$ is the actual position of the ith measurement point and $\hat{\mathbf{p}}_\mathbf{i}$ is the estimated poisition of the ith measurement point. The 3-D position estimation error of each point is shown in Fig. 8.

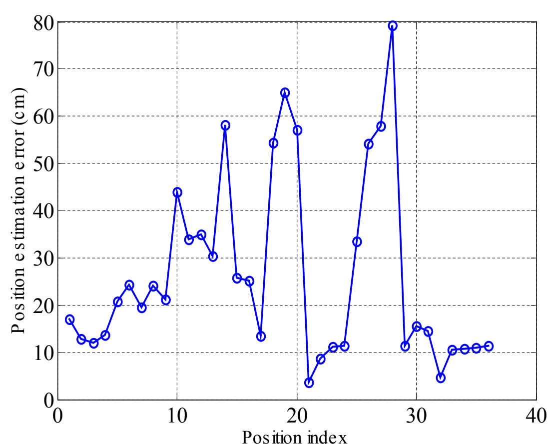

Fig. 8. Position estimation error.

For 3-D localization, the average position estimation error is 26.6 cm. The maximum position estimation error is 79.2 cm and the minimum position estimation error is 3.7 cm. There are 24 points whose position estimation error is smaller than the average error and only seven points of position estimation error greater than 50 cm. In order to increase the localization accuracy, we can either enlarge the localization unit or add more receivers to the receiver unit.

VI. Conclusion

We have introduced and analyzed a single-unit UWB 3-D localization system with the TOA technique. This system has several advantages such as no synchronization among receivers is required and easy system setup. One major effort is the derivation of the optimum receiver placement for this configuration that is not available from existing literature; we have concluded that UAA is still the optimum receiver geometry for this single-receiver-unit localization system. Another major effort is the derivation of the PEB as a function of the number of receivers and the distance between the transmitter and the receiver unit. Simulation results show that this system has the potential to provide a decimeter accuracy for 3-D localization. In order to assess the performance of this system in a realistic environment, we have constructed a hardware and software prototype system, which is tested in a laboratory. In this experiment, the transmitted UWB signal centered at 4.1 GHz has a -10 dB bandwidth of 2 GHz. Four receivers are placed inside a rectangular box, forming the receiver unit. The average position estimation errors over 36 measured locations is about couple of decimeters. The experimental results validate, to a large extent, the theoretical results obtained in this paper. The localization accuracy can be flexibly increased by enlarging the dimension of the receiver unit or by adding more receivers. This system is attractive for applications such as tracking people or objects at home, hospital, warehouse, and super market, etc.

References

[1] Multispectral solutions, Sappire DART positioning system. [Online]. Available: http://www.multispectral.com/sapphiredart.html

[2] Ubisense, Cambridge, U.K., Hardware datasheet, 2006. [Online]. Available:Http://www.ubisense.net/SITE/UPLOAD/Document/Tech-Docs/Ubisense_hardware_datasheet_May_2006.pdf.

[3] Time domain corporation website. [Online]. Available: http://timedomain.com/products/p350.pdf

[4] R. Ye, S. Redfield, and H. Liu, "High-precision indoor UWB localization: Technical challenges and method," in *Proc. 2010 IEEE ICUWB*, Sep. 2010, pp. 509–512.

[5] Institue for Inforcomm Research,Singapore, 2010. [Online]. Available: http://www.i2r.a-star.edu.sg/download.php?doc=high_precision.

[6] R. Yarlagadda, I. Ali, N. Al-Dhahir, and J. Hershey, "GPS GDOP metric," *IEE Proceedings - Radar, Sonar and Navigation,* pp. 259–264, Oct. 2000.

[7] D. Jourdan, D. Dardari, and M. Win, "Position error bound for UWB localization in dense cluttered environments," *IEEE Trans. Aerosp. Electron. Syst.*, vol. 44, pp. 613–628, Apr. 2008.

[8] B. Yang and J. Scheuing, "Cramer-Rao bound and optimum sensor array for source localization from time differences of arrival," in *Proc. IEEE ICASSP'05*, May 2005, pp. 961–964.

[9] B. Yang, "Different sensor placement strategies for TDOA based localization," in *Proc. IEEE ICASSP'07*, Apr. 2007, pp. 1093–1096.

[10] W. W. Ji and Z. Liu, "Optimum geometry selection in mobile sensor networks," in *Proc. Int. Conf. Commun. Technol.*, May 2006, vol.4, pp. 14-19

[11] J. Schroeder, S. Galler, K. Kyamakya, and K. Jobmann, "Practical considerations of optimal three-dimensional indoor localization," in *Proc. IEEE MFI'06*, Dec. 2006, pp. 439–443.

[12] K. C. Ho and L. M. Vicente, "Sensor allocation for source localization with decoupled range and bearing estimation" in *IEEE. Trans. Signal Process.*, Dec 2008, Vol.56, pp. 5773-5789

[13] Q. Zhang, W. Cao, and A. Nallanathan, "Cramér-Rao lower bounds for UWB localization with antenna array," in *Proc. IEEE ICC'10,* Cape Town, South Africa, May 2010.

[14] R. Bhatia, *Positive definite matrix*, Princeton Series in Applied Mathematics, 2007.

[15] H. V. Poor, *An introduction to signal detection and estimation*, New York: Springer-Verlag, 1994.